On-situ monitoring of sleet-thawing for OPGW based on long distance BOTDR*

LIN Rui (林睿)[1], **ZHU Yi-feng** (朱一峰)[1], **TIAN Lin** (田霖)[1], **ZHOU Li-ming** (周黎明)[2], **LIU Wei-ming** (刘伟民)[2], **and CHENG Ling-hao** (程凌浩)[2]**

1. EHV Power Transmission Company, China Southern Power Grid Co. Ltd., Guangzhou 510000, China

2. Institute of Photonics Technology, Jinan University, Guangzhou 510632, China

(Received 21 April 2020; Revised 13 July 2020)

With the absence of on-situ temperature monitoring of optical fiber composite overhead ground wire (OPGW) for the process of sleet-thawing, early temperature warning and safety control of direct current (DC) in sleet-thawing process is difficult. Here we propose a Brillouin optical time-domain reflectometry (BOTDR) with broadband receiving for fast measurement and with distributed Raman amplification for long distance measurement of about 100 km. A field experiment for on-situ temperature monitoring of sleet-thawing of OPGW is also reported, which shows uneven change of temperature along the OPGW. The difference between the maximum and the minimum temperature change can be greater than 40 °C.

Document code: A **Article ID:** 1673-1905(2021)04-0226-5

DOI https://doi.org/10.1007/s11801-021-0067-9

Special optical fiber cables of China's electric power communication transmission network are mainly composed of optical fiber composite overhead ground wire (OPGW), all-dielectric self-supporting optical cable (ADSS) and optical phase conductor (OPPC)[1-3]. Among them, OPGW is mainly used in ultra-high voltage (UHV) transmission lines, especially newly built UHV transmission lines in recent years. Ice-covered transmission lines in southern China are one of the major hidden dangers affecting the operation safety in winter[4,5]. Therefore, sleet-thawing using direct current (DC) has been proposed for OPGW to solve icing disaster of lines. By injecting DC into OPGW to increase the temperature, ice covering OPGW can melt and then be removed[6].

However, normally no temperature sensors are installed on OPGW and hence sleet-thawing process is frequently operated without on-situ temperature monitoring and control. Therefore, temperature at some places may rise much quickly than others and reach an intolerable level to damage OPGW without warning. An experiment has shown that the temperature of the fiber inside OPGW can increase to 100 °C when 366 A current was used for sleet-thawing of 25 min, which can damage the fiber and the OPGW[7]. The problem is even worse for UHV transmission lines as such lines typical span a large distance, normally over 100 km, making temperature monitoring much more difficult and OPGW more vulnerable to sleet-thawing induced over-heat[8].

As OPGW is also used for optical communications along power lines, optical fiber has already been installed in the cable. Distributed temperature sensing (DTS) based on fiber-optic technologies is then feasible[9,10]. DTS can be implemented through Raman scattering and Brillouin scattering. However, the measurement range of Brillouin scattering based schemes can be longer due to stronger scattering strength. Therefore, Brillouin scattering based DTS is more favorable for links reaching 100 km, such as those UHV lines. Brillouin DTS systems are frequently implemented through frequency scanning to analyze Brillouin gain spectrum. Because tens of frequency points are scanned sequentially, the measurement speed is slow down. The speed is even slower for longer measurement distance. For sleet-thawing monitoring of long distance UHV OPGW, the temperature changes quickly. Fast temperature measurement is therefore more favorable. Although many fiber-optic technologies have been developed for monitoring of OPGW and for ice-monitoring[11-13], the on-situ monitoring of the dynamic process of sleet-thawing for long-range OPGW is seldom reported.

In this paper, we report a long distance Brillouin optical time-domain reflectometry (BOTDR) capable of fast measurement for on-situ temperature monitoring of sleet-thawing for UHV OPGW. Distributed Raman amplification has been employed together with BOTDR to realize a long distance measurement of 100 km. Based on a scheme of broadband receiving and digital fast spectral analysis, the BOTDR can complete a measurement in

* This work has been supported by the National Natural Science Foundation of China (No.61875246).

** E-mail: chenglh@ieee.org

seconds, satisfying the demand of fast temperature measurement of sleet-thawing. The paper also reports a field experiment of a UHV OPGW link. Uneven change of temperature during sleet-thawing along the OPGW has been observed. It shows that the difference between the maximum and the minimum temperature variations can exceed 40 °C with 200 A current for sleet-thawing of one hour.

Distributed Raman amplification has been employed together with BOTDR to extent the measurement range to 100 km to meet the requirement of UHV OPGW[14,15]. Because Raman amplification is bidirectional, it amplifies the pump pulse and the Brillouin scattering signal simultaneously and hence boosts the received signal-to-noise ratio (SNR) and extents the measurement range greatly. With distributed Raman amplification, the power of the pump pulse of BOTDR increases at first due to Raman amplification, reach a peak at some position of the fiber, and then gradually drops because fiber loss is larger than Raman amplification. To extent the measurement range as far as possible, the position of power peak of the pump pulse should be also as far as possible.

If a weak signal light and a strong pump light co-propagates in a fiber and their frequency difference lies in the band of Raman gain spectrum, Raman scattering can amplify the weak signal light. Assuming the launching power of pump light at position z=0 is $P_P(0)$. Both the signal and the pump light propagate along positive direction of z-axis, the coupled propagation equations can be shown as[16]:

$$\frac{\mathrm{d}P_B(z)}{\mathrm{d}z} = \frac{g_R}{A_{eff}} P_P(z)P_B(z) - \alpha_B P_B(z), \tag{1}$$

$$\frac{\mathrm{d}P_P(z)}{\mathrm{d}z} = -\frac{v_P}{v_B}\frac{g_R}{A_{eff}} P_B(z)P_P(z) - \alpha_P P_P(z), \tag{2}$$

where $P_B(z)$ and $P_P(z)$ are the power distribution along fiber of the signal and the pump light, g_R is the Raman gain coefficient, v_B and v_P are the frequencies of the signal and the pump light, A_{eff} is the effective area of the fiber, α_B and α_P are the fiber loss of the signal and the pump light. For BOTDR system with distributed Raman amplification, the Brillouin scattering signal as the signal light is very weak compared to the Raman pump, and hence the first term at the right side of Eq.(2) can be omitted. The coupled equation can then be solved analytically. The intensity of the Brillouin scattering at position L is given by

$$P_B(z) = P_B(z)G_A\exp(-\alpha_B L), \tag{3}$$

$$G_A = \exp\left(\frac{g_R P_0 L_{eff}}{A_{eff}}\right), \tag{4}$$

$$L_{eff} = \frac{1-\exp(-\alpha_P L)}{\alpha_P}, \tag{5}$$

where P_0 is the launched power of Raman pump, G_A stands for the gain due to distributed Raman amplification. With Eqs.(3)—(5), one can obtain the maximum intensity of Brillouin scattering is at

$$L_{max} = \frac{1}{\alpha_P}\ln\frac{g_R P_0}{\alpha_B A_{eff}}. \tag{6}$$

It then shows that the loss of Brillouin scattering signal and the Raman pump should be as low as possible, and the launched power of Raman power should be as high as possible to maximize the sensing range.

The BOTDR system with distributed Raman amplification is shown in Fig.1. A narrow linewidth tunable laser operating at 1 550.12 nm is used as the source. Its output is divided into two branches. One is directed to the integrated coherent receiver (ICR) as the local oscillator (LO). The other branch is modulated by an electro-optical modulator (EOM) driven by a pulse generator to generate an optical pulse train. The bias of the EOM is manually tuned to maintain a high extinction ratio. The pulse train is amplified by an erbium doped fiber amplifier (EDFA) to a desired power level.

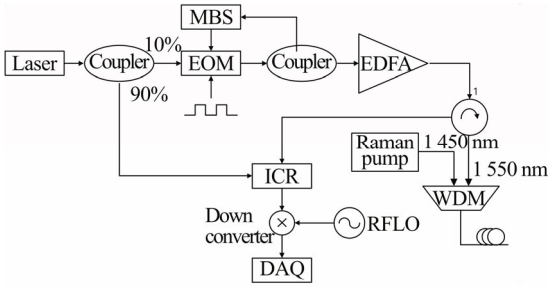

MBC: manual bias controller; EOM: electro-optical modulator; EDFA: erbium-doped fiber amplifier; ICR: intradyne coherent receiver; RFLO: radio frequency local oscillator; WDM: wavelength division multiplexer; DAQ: data acquisition

Fig.1 BOTDR system with Raman amplification

In the setup shown in Fig.1, Raman pump at 1 450 nm co-propagates with the pulse train by combing them through a wavelength division multiplexer (WDM) before launch into the sensing fiber. The Brillouin scattering signal generated at various positions of the sensing fiber is directed by the optical circulator to the signal port of the ICR and beats with the LO to generate Brillouin signal at about 10.8 GHz. This microwave signal is then downcoverted to less than 500 MHz and digitized through data acquisition for further digital processing. The sample rate here is 1 GSps.

Broadband receiving shown in Fig.1 and digital processing shown in Fig.2 is used instead of frequency scanning scheme. As shown in Fig.2, the acquired data can be processed parallelized through fast Fourier transform (FFT) to obtain Brillouin gain spectrum. In comparison, frequency scanning based methods use a passband filter with very narrow bandwidth to sample the Brillouin gain spectrum at various frequency points. Tens of frequency points are scanned sequentially to obtain a complete Brillouin gain spectrum and hence frequency scanning needs more time to complete one measurement. The cost of broadband receiving is intensive computation load.

However, parallelization can speed up the computation as shown by Fig.2 in which tens of acquired data are Fourier transformed simultaneously to obtain Brillouin gain spectrum. The resulted Brillouin gain spectrum is then summed and averaged to obtain a smooth spectrum with high SNR before Lorentz fitting to find the center frequency of the Brillouin gain spectrum. Therefore, broadband receiving with digital processing makes the measurement quicker than frequency scanning based schemes. A measurement with more than 256 averages can be completed in seconds.

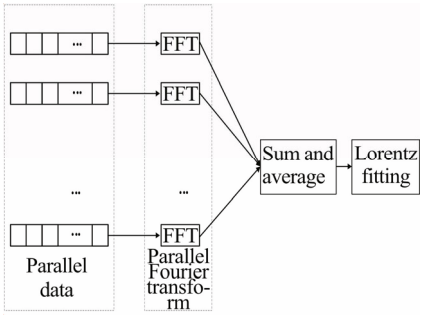

Fig.2 Digital processing to obtain the Brillouin gain spectrum

The maximum sensing range of the proposed BOTDR system can be determined through the standard deviation of measurement results. When the standard deviation of measurement results is too large at some place due to the degradation of SNR, it means the system cannot make reliable measurement and hence the sensing range reaches its limit. Therefore, sensing range is SNR dependent and hence also dependent on optical pulse power. Measurement through the proposed BOTDR system on a 125 km fiber link is then performed. The standard deviations of measurement results at various positions are calculated and shown in Fig.3 for several launched optical pulse peak power.

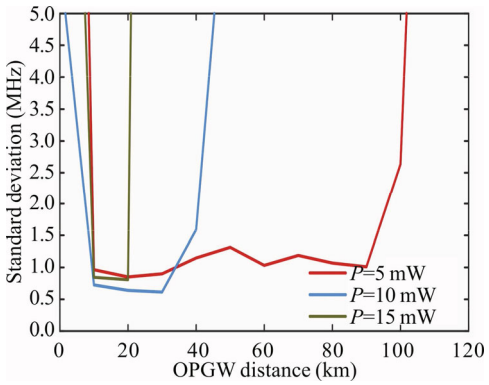

Fig.3 Standard deviation along sensing fiber for different launched optical pulse peak power

For all measurements in Fig.3, the launched optical power of the Raman pump is about 800 mW and the pulse width is 500 ns for spatial resolution of 50 m. It then shows that in the first 10 km, the standard deviation is quite large but drops quickly because in this span, the Raman amplification is still very small and the pulse power is quite weak, resulting in a very low SNR. Raman amplification increases as the pulse propagates along the fiber. Therefore, after 10 km, the standard deviation drops to a steady level of about 1 MHz. As the pulse train propagates further to some position, the standard deviation increases again. For pulse launched power of 15 mW, the standard deviation increases sharply at about 20 km. For pulse launched power of 10 mW, the sensing range is longer and can reach about 40 km. The longest sensing range is resulted by a pulse launched power of 5 mW, which reaches a standard deviation of 2.5 MHz at 100 km. It then seems that weaker pulse power leads to longer sensing range. Further investigation shows that the reason is rooted from fiber nonlinearity as elaborated below.

The measured evolution of Brillouin scattering power along fiber is shown in Fig.4. Three measurements with different launched pulse peak power, 5 mW, 10 mW and 15 mW, are shown. For the case of 5 mW, the evolution of Brillouin scattering follows the expectation of theoretical analysis given by Eqs.(1)—(6). The power gradually increase at first, reaches a peak at some place and then gradually drops. However, for the cases of 10 mW and 15 mW, the Brillouin scattering power reach peaks at places much shorter than that of 5 mW case. After the places reaching scattering peak, the scattering power drops sharply to a lower level than that of 5 mW case. It then shows that the pulse peak power for these two cases is strong enough to result in stimulated Brillouin scattering, making the pulse power depleted more quickly and the sensing range shorten greatly. For the cases of 10 mW and 15 mW, the strong pulse peak power also leads to strong self-phase modulation (SPM) induced modulation instability (MI). MI makes noise from EDFA amplified and at some place the peak of gain spectrum of MI lies in the band of Brillouin scattering. Some of this amplified noise is received through Rayleigh scattering and hence a small scattering power peak is appeared in Fig.3 for the cases of 10 mW and 15 mW. The overall effect of these fiber nonlinearities results in lower SNR after receiving and hence worse standard deviation of measurement.

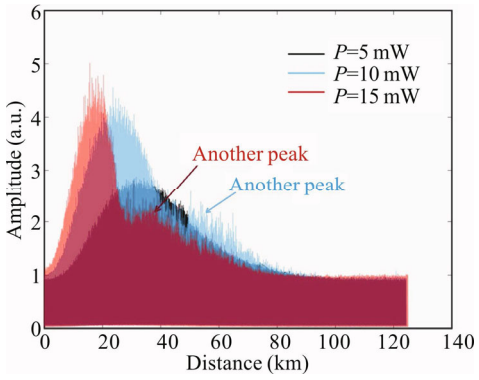

Fig.4 Measured Brillouin scattering power evolution along fiber at various pulse launched power

A field experiment to monitor the temperature distribution during sleet-thawing of a UHV OPGW link is then carried out based on the proposed BOTDR system. The link is a 500 kV UHV transmission line of 318 km without inline optical amplifier. The Brillouin frequency distribution along the OPGW link has been measured in winter and in summer, and the results for the first 35 km are shown in Fig.5. Both were measured at 8 am. Note that the Brillouin frequency shown in Fig.5 is the result after frequency down-conversion. The frequency of the local oscillator for down-conversion is 10.6 GHz and hence the original Brillouin frequency is about 10.8 GHz.

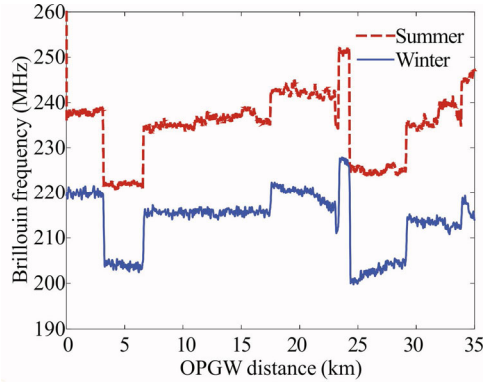

Fig.5 Brillouin center frequency distribution along the OPGW in summer and winter

The results in Fig.5 are shown as several sections with different Brillouin frequencies because different optical fibers are used in each section. Although all of the fibers in the OPGW link are standard single mode fiber, different manufactures and even different production types of the same manufacture manifest themselves in different Brillouin frequencies, which has been confirmed in laboratory. In Fig.5, there is a gap of about 16 MHz between the two curves for winter and summer to stand for the temperature difference of the two seasons and the two curves are basically parallel to each other. The temperature measured by thermometer in winter and in summer are about 4 °C and 20 °C, respectively. The gap of about 16 MHz is then related to the temperature difference in about 1°C/MHz which is in accordance with theoretical value.

A sleet-thawing through DC injection to OPGW has been done in the winter. The injection current is 200 A and the whole sleet-thawing process has lasted for an hour. The temperature distribution and variation along the OPGW link for the first 35 km has been monitored through the BOTDR system. In Fig.6, the lower curve shows the distribution after the sleet-thawing and the temperature of the OPGW has been cooled down to the environment temperature. The upper curve is basically the highest temperature distribution during sleet-thawing and shows some variation along fiber. It then shows that the amplitude of temperature change varies greatly at different positions during sleet-thawing. Fig.7 gives the difference of the highest and the lowest Brillouin frequency at various positions and hence shows the amplitude of temperature change along the OPGW link. With a temperature coefficient of 1°C /MHz for Brillouin frequency, the lowest temperature change amplitude is about 10 °C while the highest is about 53 °C. The amplitude difference is greater than 40 °C. It reveals that during sleet-thawing, the temperature change along OPGW link is very uneven. Some places may still be quite cold but other places may already be very hot. If some place is over heated, OPGW can be damaged. This uneven temperature change amplitude makes the importance of online and real-time distributed temperature monitoring prominent.

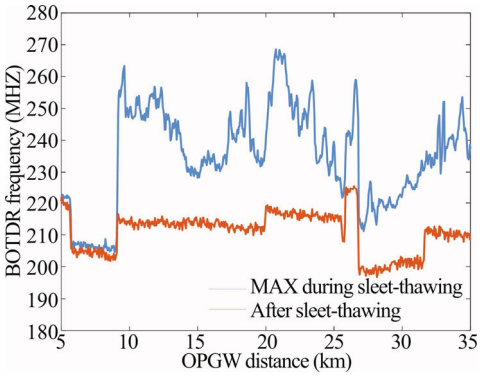

Fig.6 Brillouin frequency distribution of its maximum value during sleet-thawing and after sleet-thawing

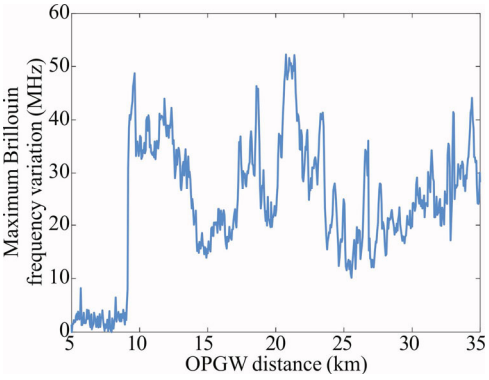

Fig.7 Distribution of maximum Brillouin frequency variation along OPGW during sleet-thawing

The temperature evolution along time at some particular place is also different from place to place. Fig.8 shows three typical measured curves of the Brillouin frequency evolution along time for three positions, which also shows the dynamic process of the sleet-thawing. At the 47th minute, the injection current is stopped and the temperature drops quickly. The entire cooling process lasts for about 10 min. But in the first 5 min, the temperature can drop about 90%. Before turning off injection current, the temperature also varies along time. The peak-to-peak variation amplitude can reach about 20 °C.

However, the behavior of such temperature variation is very different at different places. As shown in Fig.8, at position 21 248 m, the temperature of OPGW gradually increases. At 9 523 m, it gradually drops. However, at 32 666 m, the temperature does not change too much and the curve is quite flat over time. It then reflects that the temperature of OPGW is not determined by injection current alone. The local climate at which the OPGW passes by may also have great impact on the temperature of OPGW. On-situ monitoring of the dynamic temperature change of OPGW is therefore crucial to the safety of sleet-thawing operation.

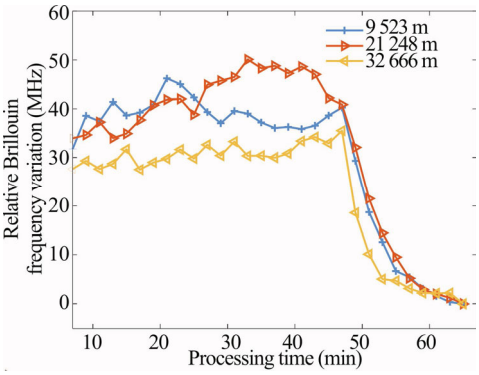

Fig.8 Brillouin frequency variation during sleet-thawing relative to its value before sleet-thawing at 3 positions

In summary, we have proposed a BOTDR system featured by broadband receiving for fast measurement. Combined with optimized distributed Raman amplification, the system can effectively measure up to 100 km in seconds. The system has been employed in on-situ monitoring of temperature distribution during sleet-thawing of an OPGW. It shows that the temperature change amplitude varies along the OPGW and the difference can greater than 40 °C. On-situ monitoring of temperature distribution is then crucial for the safety of sleet-thawing and the proposed BOTDR system can meet such requirement.

References

[1] Chai Quan, Luo Yang, Ren Jing, Zhang Jian-zhong, Yang Jun, Yuan Li-bo and Peng Gang-Ding, Optical Engineering **58**, 072007 (2019).

[2] Lu Li-dong, Sun Xiao-yan, Bu Xian-de and Li Bin-lin, Study on Passive, Wide Area and Multi-State Parameter Monitoring and Diagnosis for Power Transmission Lines, International Conference on Power System Technology (POWERCON), 2018.

[3] Ryan McMaster, A Tutorial on Optical Ground Wire Ratings Analysis for Protection Engineers, 72nd Conference for Protective Relay Engineers (CPRE), 2019.

[4] Zou Hon-liang, Tang Yi-qin, Zhang Sheng-feng, Zhao Jie, Liu Di-chen and Ma Yu-hui, Research on Ice Disaster Risk of Transmission Line Based on Annual Ice Extremum, IEEE 3rd Conference on Energy Internet and Energy System Integration (EI2), 2019.

[5] Qin Zhao-yu, Liu Wei-xin and Pan Zhe-zhe, Photoelectric Engineering **43**, 6 (2016). (in Chinese)

[6] Zhang Wei, Wu Rong-rong and Qin Wei, Southern Power System Technology **10**, 52 (2016). (in Chinese)

[7] Zhang Ye, The Application Analysis of Ice-Melting Technical Measures for OPGW, IEEE Conference on Energy Internet and Energy System Integration (EI2), 2018.

[8] Lu Jia-zheng, Hu Jian-ping, Fang Zhen and Jiang Zheng-long, High Voltage Engineering **40**, 388 (2014). (in Chinese)

[9] Abhisek Ukil, Hubert Braendle and Peter Krippner, IEEE Sensors Journal, **12**, 885 (2012).

[10] Datta A., Mamidala H., Venkitesh D. and Srinivasan B., IEEE Sensors Journal **20**, 7044 (2020).

[11] Yang Hong-lei, Liang Shi-bin, Miao Xue-peng, Cao Min and Chang Ming, Appl. Mech. Mater. **462-463**, 59 (2014).

[12] Luo Jian-bin, Hao Yan-peng, Ye Qing, Hao Yun-qi and Li Li-cheng, J. Lightwave Technol. **31**, 1559 (2013).

[13] Zhang Xu-ping, Wu Jian-ling, Shan Yuan-yuan, Liu Yang, Wang Feng and Zhang Yi-xing, Optoelectron. Technol. **37**, 221 (2017). (in Chinese)

[14] Ali Masoudi, Trevor P. Newson and Gilberto Brambilla, Long Range Distributed Optical Acoustic Sensor Based on In-Line Raman Amplification, Conference on Lasers and Electro-Optics Europe & European Quantum Electronics Conference, 2019.

[15] Xiong Ji, Wang Zi-nan, Wu Yue, Chen Yong-xiang and Rao Yun-jiang, 100km Dynamic Strain Sensing via CP-ΦOTDR, Asia Communications and Photonics Conference (ACP), 2018.

[16] Agrawal G, Nonlinear Fiber Optics, New York: Academic Press, 2005.